Wave packet dynamics in a helical optical waveguide

Stefano Longhi
Dipartimento di Fisica and Istituto di Fotonica e Nanotecnologie del CNR, Politecnico di Milano, Piazza L. da Vinci 32, I-20133 Milano, Italy
(Received 31 January 2005; published 31 May 2005)

Beam propagation in a helically twisted optical waveguide is theoretically studied and shown to provide an optical analog to the electron wave packet dynamics of a two-dimensional atom subject to a high-frequency and high-intensity circularly polarized laser field.

DOI: 10.1103/PhysRevA.71.055402 PACS number(s): 32.80.Rm, 32.80.Pj, 42.82.Et

In recent years, many interesting and unusual dynamical quantum phenomena of atoms in intense and high-frequency laser fields have been the subjected of an extended study (for reviews on this subject see, e.g., Ref. [1]). One of the most spectacular effects of laser-atom interaction in the high-frequency and high-intensity regime, which strongly deviates from the most known behavior of low-intensity laser-atom physics, is the adiabatic stabilization of the atom against ionization, i.e., an unusual increase of the atom lifetime as the laser intensity is increased [2]. Such an effect, which was predicted by Gavrila and co-workers in theoretical calculations on atomic hydrogen driven by a linearly polarized high-frequency laser field [3], can be captured by considering the electron dynamics in the Kramers–Henneberger (KH) reference frame, which is the rest frame of a classical electron in the laser field. The phenomenon of adiabatic stabilization is closely related to a strong distortion of the electronic wave packet, showing a characteristic dichotomous shape for a linearly polarized field [3] and a toroidal shape for a circularly polarized field [4]. This is due to the fact that, at high laser frequencies, the atomic core potential seen by the electron in the KH frame varies so fast that the dynamics is ruled out by a cycled-average (dressed) KH potential. Classical models, based on a phase-space analysis of classical Hamiltonian describing the electron motion subjected to either a linearly or a circularly polarized laser field, have been as well considered to explain the existence of long-lived states, and two-dimensional (2D) models for atomic hydrogen has been widely adopted to highlight the main dynamical features [5,6]. A comprehensive and accurate calculation of three-dimensional (3D) dynamic stabilization of atomic hydrogen in circularly polarized laser fields, which accounts for pulse shape effects, has been recently given in Ref. [7]. Despite a wide amount of theoretical studies on this subject has appeared in the past two decades, experimental observations of adiabatic stabilization and wave packet distortion in the atomic context are to date very few and rather indirect [1,8]. It has been recently suggested [9] and experimentally demonstrated [10] that an optical analogy of the wave packet dichotomy of an electron cloud subjected to a linearly polarized laser field, described originally by Gavrila and co-workers [3], occurs in a periodically curved optical waveguide, where beam propagation along the waveguide mimics the temporal evolution of the electronic wave function. In Refs. [9,10], a periodic bending of a waveguide on a plane was employed to simulate the effects of a linearly polarized laser field. In this paper we extend the quantum-mechanical analogy of Ref. [9] and present a 3D waveguide model which mimics the wave packet dynamics of an electron in a 2D atom [6] subjected to a *circularly polarized* laser field.

The starting point of the analysis is provided by the scalar and paraxial model for wave propagation in a channel optical waveguide, whose axis is allowed to weakly and slowly deviate from straightness; we indicate by $x=x_0(z)$ and $y=y_0(z)$ the Cartesian equations of the curved axis, where z is the direction of the straight waveguide and x,y are the transverse coordinates [see Fig. 1(a)]. As previously shown in Ref. [9], the propagation wave equation for a monochromatic light field $\psi(x,y,z)$ with a vacuum wavelength λ provides the optical analog to the semiclassical Schrödinger equation in the KH reference frame and reads explicitly

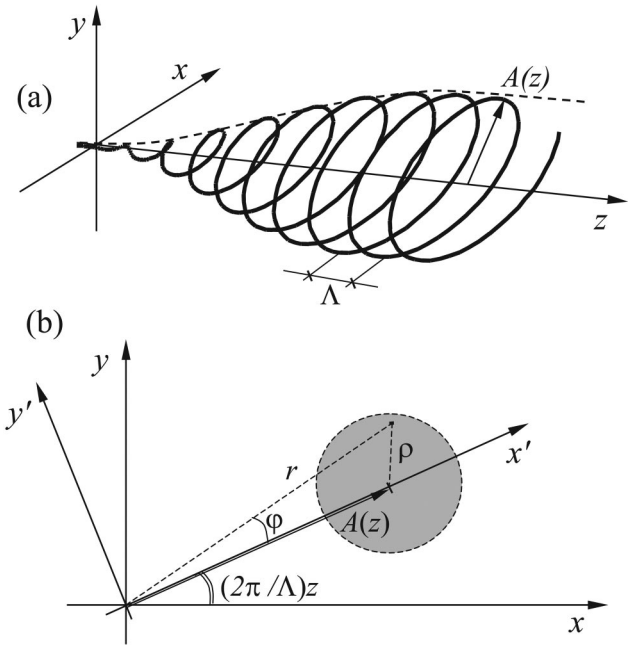

FIG. 1. (a) Schematic of a helical waveguide. (b) Rotating reference frame (x',y') used to study beam propagation in the helical waveguide. The shaded area represents the waveguide channel, i.e., the potential well $V(\rho)$ in the atomic analogy, which is centered on the x' axis at a distance $A(z)$ from the axis origin.

$$i\lambda\frac{\partial\psi}{\partial z}=-\frac{\lambda^2}{2n_s}\nabla_\perp^2\psi+V(x-x_0(z),y-y_0(z))\psi, \qquad (1)$$

where $\lambda\equiv\lambda/(2\pi)$, $V(x,y)\equiv[n_s^2-n^2(x,y)]/(2n_s)\simeq n_s-n(x,y)$, n_s is the waveguide bulk refractive index, $n(x,y)$ (with $|n(x,y)-n_s|\ll n_s$) is the transverse refractive index profile of the waveguide channel, and $\nabla_\perp^2$ is the transverse Laplacian. Note that, after the formal substitution $\lambda\to\hbar$, $z\to t$, and $n_s\to m$, Eq. (1) is equivalent to the semiclassical Schrödinger equation, in the KH frame, for a 2D electron in the binding potential $V(x,y)$, subjected to an external laser field, the terms $x_0(z)$ and $y_0(z)$ representing the quiver motion of a classical electron subjected such an external field. The optical analog corresponding to a 2D bound electron subjected to a linearly-polarized laser field was studied in Ref. [9] by considering a channel waveguide with a periodic axis bending on a plane, and the experimental observation of wave packet dichotomy associated with the adiabatic stabilization was reported in Ref. [10]. Here we focus our attention, conversely, to the optical analogy corresponding to the interaction with a *circularly polarized* laser field. To this aim, we assume that the optical waveguide has an helically twisted axis, i.e., that $x_0(z)=A\cos(2\pi z/\Lambda)$ and $y_0(z)=A\sin(2\pi z/\Lambda)$, where Λ is the spatial periodicity of the helix and A its radius. To account for a smooth turn on of the laser pulse in the atomic analogy [6], we assume that the radius of the helix A is slowly increased from zero to a constant value A_0 with a quarter sine-square rising profile [see Fig. 1(a)]. We further assume that the refractive index $n(x,y)$ of the waveguide channel has a radially symmetric shape, i.e., that $n=n(\rho)$ with $\rho=(x^2+y^2)^{1/2}$; this is in fact the most interesting case in the spirit of the quantum-optical analogy, since Eq. (1) with a radially symmetric potential exactly describes, in the optical context, 2D models for electron dynamics in atomic hydrogen subjected to a circularly polarized laser field [6]. We note that, though a 3D helical waveguide structure is unlikely achievable using common fabrication techniques, it can be obtained by the recently developed femtosecond-based microfabrication technique, which has been demonstrated to provide good-quality 3D waveguide-based photonic devices (see, for instance, Ref. [11]). To study the beam propagation dynamics along the helical waveguide, it is worth introducing a reference frame (x',y') rotating with the helical spatial periodicity; this yields the field equation

$$i\lambda\frac{\partial\psi}{\partial z}=-\frac{\lambda^2}{2n_s}\nabla_\perp'^2\psi-\frac{2\pi}{\Lambda}\mathcal{L}_z\psi+V(\rho)\psi, \qquad (2)$$

where $\mathcal{L}_z\equiv-i\lambda(x'\partial_{y'}-y'\partial_{x'})$ is the angular momentum operator along the z axis, and ρ is shown in Fig. 1(b). Note that the potential V in Eq. (2) depends implicitly, through ρ, on x' and y', but also on z owing to the slow variation of the helix radius $A(z)$ with z [see the geometric construction of Fig. 1(b)]. Note also that, once the helix radius has stabilized to its constant value A_0, V turns out to depend on x' and y' solely, leading to an autonomous (i.e., z independent) Hamiltonian. In this case, the issue of adiabatic stabilization of the atom, i.e., of low-loss light guiding along the helical structure in the optical analogy, is ultimately related to the existence of bound or quasibound states for the quantum Hamiltonian, which in turn strongly depends on the dimensionless parameter $\epsilon=\lambda/(\Lambda\Delta n)$, where Δn is the peak refractive index change of the waveguide profile. In fact, it is worth rewriting Eq. (2) in dimensionless units by rescaling the spatial variables according to $x'\to x'L_\perp$, $y'\to y'L_\perp$, $z\to zL_z$, with scales $L_\perp=\lambda(2n_s\Delta n)^{-1/2}$ and $L_z=\lambda/\Delta n$. By further introducing the polar coordinates (r,φ) [Fig. 1(b)], Eq. (2) assumes the dimensionless form

$$i\frac{\partial\psi}{\partial z}=-\nabla_\perp'^2\psi+f(r,\varphi,z)\psi+i\epsilon\frac{\partial\psi}{\partial\varphi}, \qquad (3)$$

where $f=V/\Delta n$ is the potential profile normalized to its minimum value Δn. In its present form, Eq. (3) is suited for a perturbative analysis. If we consider a constant helix radius, f is independent of z and the eigenmodes are of the form $\psi(r,\varphi,z)=F(r,\varphi)\exp(-i\beta z)$, with $(\mathcal{H}+i\epsilon\partial_\varphi)F=\beta F$ and $\mathcal{H}\equiv-\nabla_\perp'^2+f(r,\varphi)$. Depending on the value of ϵ, we have two limiting dynamical regimes. The first one occurs when $\epsilon\ll1$, i.e., the long helix period regime. In this regime, F and β can be constructed by means of standard perturbation analysis starting from an unperturbed bound mode of the Hamiltonian $\mathcal{H}$. Therefore, in the (x,y) laboratory reference frame, we expect the helical waveguide to guide, with low losses, the modes of the straight waveguide—slightly perturbed by the bending—which adiabatically follow the helical axis trajectory. The other limiting dynamical regime, which is analogous to the high-frequency limit in the atomic analogy, corresponds to a short helix period, i.e., to $\epsilon\gg1$. In this case, one can develop a stationary perturbation analysis in power series of the small parameter $1/\epsilon$, yielding at leading order $\beta=\epsilon\, l+\beta_0$ and $F(r,\varphi)=R(r)\exp(-il\varphi)$, where l is the azimuthal index, related to the beam angular momentum, and R and β_0 satisfy the radial eigenvalue equation

$$-\frac{1}{r}\frac{\partial}{\partial r}\left(r\frac{\partial R}{\partial r}\right)+\frac{l^2}{r^2}R+f_{\mathrm{av}}(r)R=\beta_0 R, \qquad (4)$$

where $f_{\mathrm{av}}(r)=1/(2\pi)\int_0^{2\pi}d\varphi f(r,\varphi)$ is the averaged potential over the angular coordinate. We, hence, expect the waveguide to guide, with low losses, the modes of a straight waveguide which, in the laboratory (x,y) reference frame, shows a refractive index profile given by the cycled-averaged refractive index of the helical waveguide. We also note that, if we include the slow dependence of the potential f on z due to the adiabatic increase of the helix radius $A(z)$ from zero to the constant value A_0 [see Fig. 1(a)], in the limit $\epsilon\to\infty$ the following cycled-averaged wave equation can be derived form Eq. (3) by a multiple scale analysis (see, e.g., Ref. [9] for technical details)

$$i\frac{\partial\psi}{\partial z}=-\nabla_\perp'^2\psi+f_{\mathrm{av}}(r,z)\psi+i\epsilon\frac{\partial\psi}{\partial\varphi}, \qquad (5)$$

where $f_{\mathrm{av}}(r,z)=1/(2\pi)\int_0^{2\pi}d\varphi\, f(r,\varphi,z)$. It is clear that, if the helix radius becomes comparable or larger than the radial size of the potential f, the angle-averaged potential f_{av} has an annular profile, with a depressed refractive index in the inner

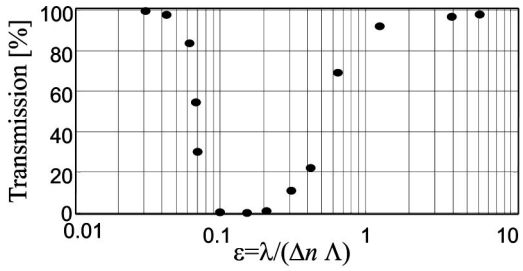

FIG. 2. Power transmission vs ϵ for a $L=1000$ long (in units L_z) helical waveguide with a Gaussian-shaped refractive index profile. Parameter values are $a=6.3246$ and $A_0=25.3$ (in units $L_\perp$).

and outer parts of a ring of radius $r \simeq A_0$, so that the modes guided by the helically twisted waveguide in the short-period limit are those of an annular (or tubular) waveguide (see, for instance, Ref. [12]). It is also interesting to note that, since within the average waveguide model (5) the angular momentum operator $\mathcal{L}_z=-i\partial_\varphi$ commutes with the Hamiltonian $-\nabla'^2_\perp+f_{\rm av}(r,z)+i\partial_\varphi$, one has $d\langle\mathcal{L}_z\rangle/dz=0$, i.e., the mean value of the angular beam momentum is conserved during the propagation. In the operational conditions corresponding to a finite value for ϵ, strong radiation losses may occur, and a direct integration of Eq. (1) over a finite transverse domain with absorbing boundary conditions is needed to determine radiation losses (see Ref. [9]). We numerically integrated Eq. (1) using a pseudospectral beam propagation method on a square transverse domain with absorbing boundary conditions assuming, as an example, a Gaussian profile for the potential well, $V(\rho)\simeq n_s-n(x,y)=-\Delta n\exp(-\rho^2/a^2)$. Analogously to the lifetime calculation of atomic hydrogen subjected to a strong laser field [6], the beam power $\mathcal{P}(z)=\int|\psi(x,y)|^2dxdy$ contained in the finite transverse integration domain can be used to quantitatively measure radiation losses, i.e., the ionization probability of the atom in the quantum-mechanical context. We numerically computed the power transmission of the helical waveguide of length L, $\mathcal{P}(L)/\mathcal{P}(0)$, as a function of the dimensionless parameter $\epsilon=\lambda/(\Lambda\Delta n)$ and helix radius A_0, scaled to $L_\perp=\lambda(2n_s\Delta n)^{-1/2}$. A waveguide length $L=1000L_z$ has been assumed, with a 20% initial stage in which the helix radius adiabatically increases, through a quarter sine-square ramp, from zero to its final value A_0 [see Fig. 1(a)]. The waveguide was excited in its fundamental radially symmetric mode [13]. Figure 2 shows the behavior of beam power transmission vs ϵ for a fixed value of the helix radius. Note that, according to the perturbative analysis, low losses are found for small or large values of ϵ, with a connecting region where the guiding properties of the helical waveguide are fully lost. The large ϵ limit corresponds to the high-frequency adiabatic stabilization regime, in which beam propagation is well described by the "average" waveguide wave equation (5). This is shown in Fig. 3, where an example of beam propagation in the adiabatic stabilization regime is depicted; note the appearance of a stabilized annular-shaped wave packet after the adiabatic waveguide section, which resembles the electron wave form of a 2D hydrogen atom subjected to a circularly polarized field [6]. In terms of real-world physical parameters, for a peak refractive index change $\Delta n=0.01$, a substrate refractive

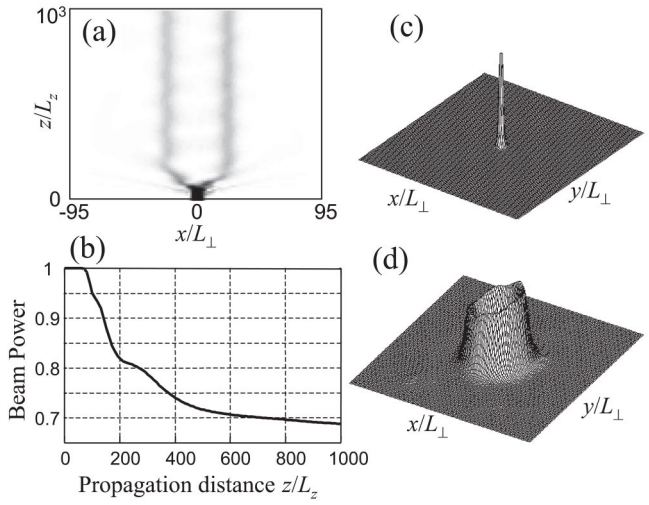

FIG. 3. Beam dynamics along a helical waveguide, showing adiabatic beam stabilization. (a) Gray-scale plot of beam amplitude $|\psi|$ on the $y=0$ plane; (b) Evolution of beam power $\mathcal{P}$; (c) Intensity profile $|\psi|^2$ of injected fundamental waveguide mode [13]; (d) Intensity beam profile at the output of the waveguide. The square transverse domain is 190×190 wide (in units $L_\perp$). Parameter values are $A_0=25.3L_\perp$ and $\epsilon=\pi/5$; the other parameter values are the same as in Fig. 2.

index $n_s=1.5$ and for a probing wavelength $\lambda=1.55$ μm, the waveguide shown in Fig. 3 corresponds to a total length $L\simeq24.67$ mm, a helix period $\Lambda\simeq246.7$ μm, a helix radius $A_0\simeq36$ μm, and a transverse size of the waveguide channel $a\simeq9$ μm; the transverse and longitudinal spatial scales are then $L_\perp=1.46$ μm and $L_z=24.67$ μm, respectively. The well-known phenomenon of adiabatic stabilization and ionization quenching [6] is shown in Fig. 4, where beam power transmission vs helix radius amplitude A_0 is depicted for a fixed value of ϵ [14]. Note that, when A_0 is smaller than the characteristic size a of the potential $V(\rho)$, as A_0 increases radiation losses increase; however, at higher values of A_0, corresponding to the appearance of an annular-shaped averaged potential $f_{\rm av}$, the beam power transmission increases as A_0 is increased.

In summary, we proposed a 3D helical optical waveguide model to mimic, in an optical system, the electron wave function dynamics of a 2D atom subjected to a high-frequency and high-intensity circularly polarized laser field.

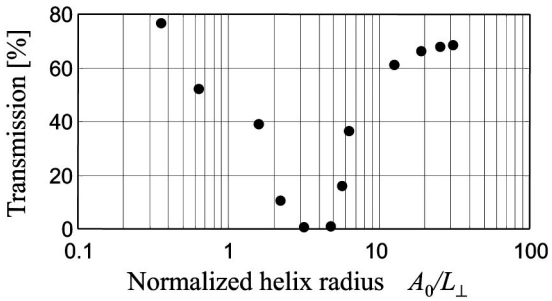

FIG. 4. Power transmission vs dimensionless helix radius $A_0/L_\perp$ for $\epsilon=\pi/5$. The values of other parameters are the same as in Fig. 2.

The optical analogy may be of relevance for an experimentally accessible study of adiabatic stabilization and annular wave function distortion phenomena which are not easily accessible to date in the atom-laser physics context. It is also envisaged that, within the ray-optics limit $\lambda \to 0$, the helical waveguide system may also provide a way to study the complex classical dynamics of hydrogen atoms in circularly polarized laser fields [6].

[1] M. Gavrila, in *Atoms in Intense Laser Fields*, edited by M. Gavrila (Academic, New York, 1992), p. 435; K. Burnett, V. C. Reed, and P. L. Knight, J. Phys. B **26**, 561 (1993); M. Protopapas, C. H. Keitel, and P. L. Knight, Rep. Prog. Phys. **60**, 389 (1997); M. Gavrila, J. Phys. B **35**, R147 (2002).

[2] M. Pont and M. Gavrila, Phys. Rev. Lett. **65**, 2362 (1990).

[3] M. Pont, N. R. Walet, M. Gavrila, and C. W. McCurdy, Phys. Rev. Lett. **61**, 939 (1988).

[4] M. Pont, Phys. Rev. A **40**, 5659 (1989).

[5] J. Javanainen, J. H. Eberly, and Q. Su, Phys. Rev. A **38**, 3430 (1988); R. V. Jensen and B. Sundaram, Phys. Rev. Lett. **65**, 1964 (1990); A. F. Brunello, T. Uzer, and D. Farrelly, Phys. Rev. A **55**, 3730 (1997).

[6] W. Chism, D. I. Choi, and L. E. Reichl, Phys. Rev. A **61**, 054702 (2000); E. Okon, W. Parker, W. Chism, and L. E. Reichl, *ibid.* **66**, 053406 (2002).

[7] M Boca, H. G. Muller, and M Gavrila, J. Phys. B **37**, 147 (2004).

[8] M. P. de Boer, J. H. Hoogenraad, R. B. Vrijen, L. D. Noordam, and H. G. Muller, Phys. Rev. Lett. **71**, 3263 (1993); N. J. van Druten, R. C. Constantinescu, J. M. Schins, H. Nieuwenhuize, and H. G. Muller, Phys. Rev. A **55**, 622 (1997).

[9] S. Longhi, D. Janner, M. Marano, and P. Laporta, Phys. Rev. E **67**, 036601 (2003).

[10] S. Longhi, M. Marangoni, D. Janner, R. Ramponi, P. Laporta, E. Cianci, and V. Foglietti, Phys. Rev. Lett. **94**, 073002 (2005).

[11] K. Minoshima, A. M. Kowalevicz, I. Hartl, E. P. Ippen, and J. G. Fujimoto, Opt. Lett. **26**, 1516 (2001).

[12] A. Zoubir, C. Lopez, M. Richardson and K. Richardson, Opt. Lett. **29**, 1840 (2004).

[13] For parameter values used in the numerical simulations, the straight waveguide turns out to be multimode. The guided TEM_{nl} modes, where n and l are the radial and azimuthal mode numbers, are precisely: TEM_{00} (the radially invariant fundamental waveguide mode), TEM_{10}, TEM_{20}, TEM_{30}, TEM_{01}, TEM_{11}, TEM_{02}, and TEM_{03}.

[14] The helix radius A_0 plays the same role as the laser field intensity in the atomic context, whereas the dimensionless parameter ϵ, which is inversely proportional to the helix period Λ, is analogous to the laser frequency.